STEM CELLS®

CANCER STEM CELLS

Evidence for Transcriptional Regulation of the Glucose-6-Phosphate Transporter by HIF-1α: Targeting G6PT with Mumbaistatin Analogs in Hypoxic Mesenchymal Stromal Cells

SIMON LORD-DUFOUR,[a] IAN B. COPLAND,[b] LOUIS-CHARLES LEVROS JR.,[c] MARTIN POST,[d] ABHIRUP DAS,[e] CHAITAN KHOSLA,[e] JACQUES GALIPEAU,[b] ERIC RASSART,[c] BORHANE ANNABI[a]

[a]Laboratoire d'Oncologie Moléculaire, Département de Chimie, Centre BIOMED, and [c]Laboratoire de Biologie Moléculaire, Département des Sciences Biologiques, Université du Québec à Montréal, Quebec, Canada; [b]Department of Medicine, Lady Davis Institute for Medical Research, Montreal, Quebec, Canada; [d]Lung Biology Research Program, The Hospital for Sick Children Research Institute, Toronto, Ontario, Canada; [e]Departments of Chemistry, Chemical Engineering, and Biochemistry, Stanford University, Stanford, California, USA

Key Words. Mesenchymal stromal cells • Hypoxia inducible factor-1 alpha • Glucose-6-phosphate transporter • Stem cell migration • Brain tumor

ABSTRACT

Mesenchymal stromal cell (MSC) markers are expressed on brain tumor-initiating cells involved in the development of hypoxic glioblastoma. Given that MSCs can survive hypoxia and that the glucose-6-phosphate transporter (G6PT) provides metabolic control that contributes to MSC mobilization and survival, we investigated the effects of low oxygen (1.2% O_2) exposure on *G6PT* gene expression. We found that MSCs significantly expressed G6PT and the glucose-6-phosphatase catalytic subunit β, whereas expression of the glucose-6-phosphatase catalytic subunit α and the islet-specific glucose-6-phosphatase catalytic subunit-related protein was low to undetectable. Analysis of the G6PT promoter sequence revealed potential binding sites for hypoxia inducible factor (HIF)-1α and for the aryl hydrocarbon receptor (AhR) and its dimerization partner, the AhR nuclear translocator (ARNT), AhR:ARNT. In agreement with this, hypoxia and the hypoxia mimetic cobalt chloride induced the expression of G6PT, vascular endothelial growth factor (VEGF), and HIF-1α. Gene silencing of *HIF-1α* prevented G6PT and VEGF induction in hypoxic MSCs whereas generation of cells stably expressing HIF-1α resulted in increased endogenous *G6PT* gene expression. A semisynthetic analog of the polyketide mumbaistatin, a potent G6PT inhibitor, specifically reduced MSC-HIF-1α cell survival. Collectively, our data suggest that G6PT may account for the metabolic flexibility that enables MSCs to survive under conditions characterized by hypoxia and could be specifically targeted within developing tumors. STEM CELLS *2009;27:489–497*

Disclosure of potential conflicts of interest is found at the end of this article.

INTRODUCTION

Molecular markers associated with mesenchymal stromal cells (MSCs) are thought to characterize the brain tumor-initiating cells involved in the development of glioblastoma, the most common and aggressive primary brain cancer [1]. Given that glioblastomas are also highly hypoxic tumors [2], these findings suggest that a subset of primary glioblastomas may be derived from transformed stem cells having MSC-like properties and retaining partial phenotypic aspects of the MSC nature within the tumors' hypoxic environment. Bone marrow-derived MSCs are a population of pluripotent adherent cells residing within the bone marrow microenvironment that can differentiate into many mesenchymal phenotypes [3, 4]. Interestingly, the recruitment of MSCs by experimental vascularizing tumors has resulted in the incorporation of MSCs within the tumor architecture [5, 6], which implies that these cells must respond to tumor-derived growth factor cues [7, 8]. More importantly, their potential contribution to tumor development also implies that MSCs must adapt to the low oxygen environment and nutrient deprivation that characterizes hypoxic tumors.

MSCs were recently demonstrated to also have the capacity to survive under conditions of ischemia and to resist

Author contributions: S.L.-D.: collection and assembly of data, data analysis, manuscript writing; I.B.C.: collection and assembly of data, manuscript writing; L.-C.L.: collection and assembly of data; M.P.: collection and assembly of data; A.D.: collection and assembly of data; C.K.: data analysis, manuscript writing; J.G.: collection of data, data analysis, manuscript writing; E.R.: data analysis, manuscript writing; B.A.: conception and design, data analysis, manuscript writing, financial support.

Correspondence: Borhane Annabi, Ph.D., Laboratoire d'Oncologie Moléculaire, Université du Québec à Montréal, C.P. 8888, Succersale Centre-Ville, Montréal, Québec, Canada, H3C 3P8. Telephone: 514-987-3000, ext. 7610; Fax: 514-987-0246; e-mail: annabi.borhane@uqam.ca Received August 28, 2008; accepted for publication December 3, 2008; first published online in STEM CELLS *EXPRESS* December 11, 2008. 1066-5099/2009/$30.00/0 doi: 10.1634/stemcells.2008-0855

hypoxic culture conditions [9]. Furthermore, resistance of MSCs to inhibition of mitochondrial respiration also indicates that MSCs can survive in the absence of oxygen using both anaerobic ATP production and increased glycolysis [9]. The control of glycolysis and of gluconeogenesis occurs primarily at the level of the interconversion of fructose-6-phosphate and fructose-1,6-bisphosphate under the action of phosphofructokinase-1 (PFK-1) and fructose-1,6-bisphosphatase [10]. Increased glycolysis is essential for the survival and spread of cancer cells in a low oxygen environment. Under these conditions, the key step in controlling the glycolytic rate involves PFK-1, whose activation is controlled by the hypoxia-inducible factor (HIF)-1 complex [11]. HIF-1 is a transcription factor that is induced during the adaptation of tumor cells to hypoxia, activating the transcription of genes that, in turn, regulate several biological processes, including angiogenesis, cell proliferation and survival, glucose metabolism, pH regulation, and migration [12]. HIF-1α, the oxygen-sensitive subunit of HIF-1, was shown to induce the recruitment of bone marrow-derived vascular modulatory cells and trigger processes involved in tumor angiogenesis and invasion [13]. It also regulates homing of marrow-derived progenitor cells to injured tissue [14]. Whether alternate intracellular metabolic systems, such as the glucose-6-phosphatase (G6Pase) system, would enable MSCs to survive under conditions of hypoxic stress and whether these systems would be regulated by the HIF-1 complex are currently unknown.

Recently, impaired chemotaxis was reported in bone marrow cells isolated from a G6PT deficient ($G6PT^{-/-}$) mouse [15, 16]. In agreement with those reports, we have demonstrated that G6PT can regulate cell migration [17] as well as MSC chemotaxis and survival [18]. In fact, since its discovery, G6PT has been shown to be responsible for G6P transport from the cytosol to the lumen of the endoplasmic reticulum (ER), therefore performing the rate-limiting step for G6P hydrolysis into glucose and inorganic phosphate by the G6Pase system. G6PT has been shown to integrate and regulate many metabolic functions such as glycemia, lipidemia, uricemia, and lactic acidemia [19]. More importantly, its activity cannot be substituted because G6PT deficiencies lead to glycogen storage disease (GSD) type Ib, characterized not only by disturbed glucose homeostasis but by severe myeloid dysfunction [19]. Besides MSCs, G6PT is believed to play a role in neutrophil chemotaxis and calcium flux control [20–23], and in U87 glioma cell survival [24, 25]. In turn, *G6PT* gene expression is regulated in response to adaptive metabolic changes involving glucose, insulin, and cyclic AMP [26]. In this study, we investigated whether transcription of G6PT could be further regulated under the control of hypoxia-responsive elements, and to what extent G6PT could promote MSC survival under hypoxic conditions.

Materials and Methods

Materials

SDS and bovine serum albumin (BSA) were purchased from Sigma (Oakville, ON, Canada, http://www.sigmaaldrich.com). Cell culture media were obtained from Life Technologies (Burlington, ON, Canada, http://www.lifetech.com). Electrophoresis reagents were purchased from Bio-Rad (Mississauga, ON, Canada, http://www.bio-rad.com). The enhanced chemiluminescence reagents were from Amersham Pharmacia Biotech (Baie d'Urfé, QC, Canada, http://www.amersham.com). Micro bicinchoninic acid protein assay reagents were from Pierce (Rockford, IL, http://www.piercenet.com). The polyclonal antibodies against HIF-1α and poly-(ADP-ribose) polymerase (PARP) were from Chemicon (Temecula, CA, http://www.chemicon.com). The polyclonal antibodies against phospho-AKT, phospho-extracellular signal related kinase (ERK), and glyceraldehyde-3-phosphate dehydrogenase (GAPDH) were purchased from Cell Signaling Technology, Inc. (Danvers, MA, http://www.cellsignal.com).

Cell Culture and Experimental Hypoxic Conditions

Bone marrow-derived MSCs were isolated from the whole femur and tibia bone marrow of C57BL/6 female mice; cells were cultured and characterized as previously described [27]. Analysis by flow cytometry, performed at passage 14, revealed that MSCs expressed CD44 yet were negative for CD45, CD31, KDR/flk1 (vascular endothelial growth factor receptor [VEGFR]-2), flt-4 (VEGFR-3), and Tie2 (angiopoietin receptor) (data not shown). Cells were cultured in serum-free Dulbecco's modified Eagle's medium during drug treatment in order to approximate the pathophysiological conditions of low growth factors and nutrient availability such as that found within the hypoxic environment of developing tumors. Hypoxic conditions were attained by incubation of confluent cells in an anaerobic box. The oxygen was maintained at 1% by a compact gas oxygen controller, Proox model 110 (BioSpherix, Redfield, NY, http://www.biospherix.com), with a residual gas mixture composed of 94% N_2 and 5% CO_2.

cDNA Construct Generation and Transduction of MSC-HIF-1α Cells

The human full-length HIF-1α cDNA construct was generously provided by Dr. Semenza (Johns Hopkins University, Baltimore, MD) and was used as a template for generating an *HIF-1α* mutant that lacked its oxygen-dependent degradation domain ($ODD_{401\text{-}603}$). The deletion mutant (HIF-1α ΔODD) was constructed by overlap extension using polymerase chain reaction (PCR). The deletion was confirmed by DNA sequencing, and the 1.95-kb HIF-1α ΔODD cDNA was subcloned into pcDNA3.1. For generation of retroviral particles, the HIF-1α ΔODD construct was digested out of the pcDNA3.1 vector using BamHI and HpaI restriction enzymes and subcloned into the multiple cloning site of the bicistronic retrovector internal ribosomal entry segment–green fluorescent protein plasmid (pIRES-GFP). 293-GP2 viral packaging cells were transfected with either the HIF-1α ΔODD-pIRES-GFP or null-pIRES-GFP plasmids, and the viral supernatant was collected at 48 and 72 hours post-transfection. MSCs were subjected to eight rounds of viral transduction. Following viral transduction, each GFP^+ MSC (AP2-MSC) and HIF-1α ΔODD-GFP^+ MSC population was subjected to high-speed cell sorting (BD FacsAria; BD Biosciences, San Diego, http://www.bdbiosciences.com) to obtain polyclonal pooled clones of retrovirally transfected MSCs that were 100% GFP^+ and similar in regard to GFP signal intensity.

Immunoblotting Procedures

Nuclear extracts from MSCs or MSC-HIF-1α cells were isolated using the NE-PER Nuclear and cytoplasmic extraction kit (Pierce) and proteins were separated by SDS-PAGE. After electrophoresis, proteins were electrotransferred to polyvinylidene difluoride membranes, which were then blocked for 1 hour at room temperature with 5% nonfat dry milk in Tris-buffered saline (150 mM NaCl, 20 mM Tris–HCl, pH 7.5) containing 0.3% Tween-20 (TBST). Membranes were further washed in TBST and incubated with the anti-HIF-1α primary antibody (1/1,000 dilution) in TBST containing 3% BSA, followed by a 1-hour incubation with horseradish peroxidase-conjugated anti-rabbit IgG in TBST containing 5% nonfat dry milk. Immunoreactive material was visualized by enhanced chemiluminescence (Amersham).

Cell Migration Assay

MSCs or MSC-HIF-1α cells were trypsinized and seeded at 10^5 cells on 0.15% gelatin/phosphate-buffered saline precoated

Transwells (8-μm pore size; Corning/Costar, Acton, MA, http://www.corning.com/lifesciences) assembled in 24-well Boyden chambers that were filled with 600 μl of serum-free medium. Cell migration was allowed to proceed for 6 hours at 37°C in 5% CO_2. Nonmigrating cells that remained on the upper side of the Transwell filter were carefully removed with cotton swabs. Cells that had migrated to the lower side of the filters were fixed with 3.7% formaldehyde and stained with 0.1% crystal violet/20% MeOH and counted. The migration was quantified by analyzing at least 10 random fields per filter for each independent experiment using the computer-assisted imaging software Northern Eclipse 6.0 (Empix Imaging Inc., Mississauga, ON, Canada, http://www.empix.com).

Total RNA Isolation, cDNA Synthesis, and Real-Time Quantitative Reverse Transcription-PCR

Total RNA was extracted from MSC monolayers using TRIzol reagent (Life Technologies, Gaithersburg, MD, http://www.lifetech.com). For cDNA synthesis, 1 μg of total RNA was reverse-transcribed into cDNA using a high-capacity cDNA reverse transcription (RT) kit (Applied Biosystems, Foster City, CA, http://www.appliedbiosystems.com). cDNA was stored at −80°C prior to PCR. Gene expression was quantified by real-time quantitative (q)PCR using iQ SYBR Green Supermix (Bio-Rad, Hercules, CA, http://www.bio-rad.com). DNA amplification was carried out using an Icycler iQ5 (Bio-Rad) and product detection was performed by measuring binding of the fluorescent dye SYBR Green I to double-stranded DNA. All the QuantiTect primer sets were provided by Qiagen (Valencia, CA http://www1.qiagen.com): Mm_Hif1a_1_SG QT01039542, Mm_Slc37a4_1_SG QT00124411, Mm_G6pc_1_SG (NM_008061) QT00114625, Mm_G6pc2_1_SG (NM_021331) QT00139461, and Mm_G6pc3_1_SG (NM_175935) QT00104748. The relative quantities of target gene mRNA against an internal control, 18S ribosomal RNA, were measured by following a [/delta]C_T method employing an amplification plot (fluorescence signal versus cycle number). The difference ([/delta]C_T) between the mean values in the triplicate samples of target gene and those of 18S ribosomal RNA was calculated by iQ5 Optical System Software version 2.0 (Bio-Rad) and the relative quantified value was expressed as $2_T^{-/\delta C}$.

Semiquantitative RT-PCR Analysis

One microgram of total RNA was used for first-strand cDNA synthesis followed by specific gene product amplification with the One-Step RT-PCR kit (Invitrogen, Carlsbad, CA, http://www.invitrogen.com). The primers used were the same as for the qRT-PCR and were all derived from mouse sequences. GAPDH cDNA amplification was used as an internal housekeeping gene control. PCR conditions were optimized so that the gene products were examined at the exponential phase of their amplification and the products were resolved on 2.2% agarose gels containing 1 μg/ml ethidium bromide.

Transfection Method and RNA Interference

MSCs were transiently transfected with 20 μM small interfering (si)RNA against HIF-1α (Mm_Hif1a_1 HP siRNA, SI00193011) using HiPerFect (Qiagen). HIF-1α-specific gene knockdown was evaluated by qRT-PCR as described above. siRNA against HIF-1α and mismatch siRNA were synthesized by Qiagen and annealed to form duplexes.

Morphological Analysis of Apoptotic and Necrotic Cells

To visualize nuclear morphology and chromatin condensation by fluorescence microscopy [18], cells were pretreated for 18 hours with chlorogenic acid (CHL), the mumbaistatin analog (AD4-015), or their respective vehicle (ethanol or dimethylsulfoxide). Cells were stained with 0.06 mg/ml Hoechst (33258, blue fluorescence) for apoptotic cells or with 50 μg/ml propidium iodide (PI) (red fluorescence) for necrotic cells. Observations were made by fluorescence microscopy (Carl Zeiss Ltd, Montreal, QC, Canada, http://www.zeiss.com) and photographs were taken with a digital camera (camera 3CCD, Sony DXC-950P, Empix Imaging Inc.). Images were analyzed by Northern Eclipse software. A minimum of 600 cells was counted per dish.

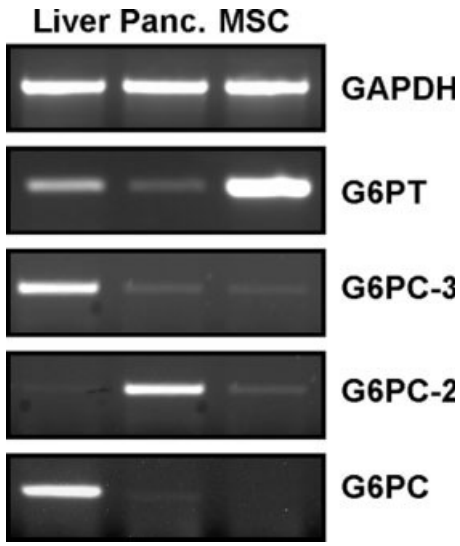

Figure 1. Murine mesenchymal stromal cells (MSCs) strongly express the glucose-6-phosphate transporter (G6PT) component of the glucose-6-phosphatase system. Total RNA was extracted from mouse MSCs, mouse liver, and mouse pancreas as described in the Methods section. cDNA synthesis and semiquantitative reverse transcription-polymerase chain reaction were performed to assess gene expression of G6PT, the glucose-6-phosphatase catalytic subunit α (G6PC), the islet-specific glucose-6-phosphatase catalytic subunit-related protein (G6PC-2), and the glucose-6-phosphatase catalytic subunit β (G6PC-3).

Electrophoretic Mobility Shift Assays

Fifty nanograms of sense oligonucleotide was 5′-end-labeled with T4 polynucleotide kinase and [γ-^{32}P]ATP and annealed with 200 ng of the complementary oligonucleotide. Nuclear extracts from growing MSC-HIF-1α cells were prepared according to the method of Dignam et al. [28]. Nuclear extracts were analyzed by gel shift assays as described previously [29]. Thirty micrograms of nuclear extract was added to 0.8 ng of the labeled double-stranded oligonucleotide, and, after a 20-minute incubation at room temperature, the mixture was run on a 6% acrylamide, nondenaturing gel in 0.5 × Tris/Borate/EDTA at 150 V for 90 minutes. The dried gels were autoradiographed on Kodak X-Omat films (Sigma). For competition assays, a 25-fold excess (20 ng) of cold double-stranded oligonucleotide was added before addition of the nuclear extract. The sense strand sequences of the oligonucleotides used are: HIF-1α, CCG AGG CTA CGT GCG GCT TCT CTC G; nonspecific competitor (NSC) (unrelated sequence), CCA AAC AGG ATA TCT GTA ATA AGC AG.

Results

Murine MSCs Strongly Express the G6PT Component of the G6Pase System

In order to confirm expression of the G6PT component in MSCs, semiquantitative RT-PCR was performed using total RNA extracted from mouse MSCs, mouse liver, and mouse pancreas. Measurement of the other three components of the G6Pase system—the glucose-6-phosphatase catalytic subunit α (G6PC), the islet-specific glucose-6-phosphatase catalytic

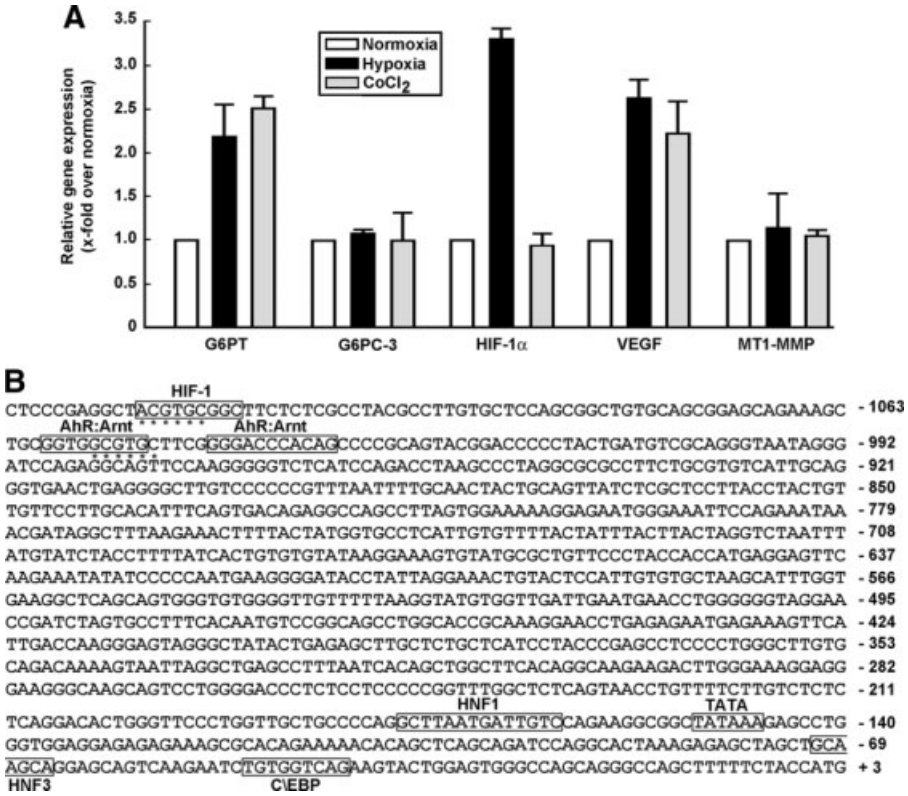

Figure 2. Cobalt chloride-induced chemical hypoxia and hypoxic culture conditions regulate *G6PT* gene expression. **(A):** Subconfluent mesenchymal stromal cells were serum-starved and cultured under normoxic (5% CO_2 and 95% air; white box) or hypoxic (1% O_2, 5% CO_2, and 94% N_2; black box) conditions, or treated with 100 μM $CoCl_2$ (gray box) for 18 hours. Total RNA was extracted and quantitative reverse transcription-polymerase chain reaction was performed in order to assess *G6PT*, *G6PC-3*, *HIF-1α*, *VEGF*, and *MT1-MMP* gene expression levels. **(B):** A 1,133-bp sequence upstream of the ATG coding sequence of the murine *G6PT* gene promoter sequence, located on mouse chromosome nine at location 44,205,182-44,211,045, was analyzed (National Center for Biotechnology Information source NM_008063.2). The core consensus sequence of the hypoxia responsive elements (A_G)CGT(G_C)C is denoted by asterisks [50, 51]. Sequences of a TATA box (−152/−147) and potential binding sites for HIF-1 (−1122/−1114), AhR:Arnt (−1059/−1051 and −1045/−1035), HNF1 (−177/−164), HNF3 (−71/−65), and C/EBP (−48/−40) are boxed. Abbreviations: AhR, aryl hydrocarbon receptor; Arnt, AhR nuclear translocator; C/EBP, CCAAT/enhancer binding protein; G6PC-3, glucose-6-phosphatase catalytic subunit β; G6PT, glucose-6-phosphate transporter; HIF-1α, hypoxia inducible factor 1α; HNF, hepatocyte nuclear factor; MT1-MMP, membrane type-1 matrix metalloproteinase; VEGF, vascular endothelial growth factor.

subunit-related protein (G6PC-2), and the glucose-6-phosphatase catalytic subunit β (G6PC-3)—was also performed. Compared with liver or pancreas, MSCs significantly expressed G6PT. In contrast, G6PC and G6PC-3 were expressed at low to undetectable levels in MSCs and pancreas in comparison with liver. As expected, *G6PC-2* gene expression was clearly detected in pancreas, whereas its expression was very low in MSCs and undetectable in liver (Fig. 1). GAPDH served as an internal loading control and remained constant. In contrast to hepatocytes, which predominantly utilize α-ketoacids as fuel, MSCs may presumably heavily depend on G6P for their energy needs.

Cobalt Chloride-Induced Chemical Hypoxia and Hypoxic Culture Conditions Regulate *G6PT* Gene Expression

MSCs were serum-starved and cultured under hypoxic conditions (18 hours under 1.2% O_2) or treated with cobalt chloride ($CoCl_2$), a condition known to mimic hypoxic culture conditions. Total RNA was extracted and qRT-PCR was performed as described in the Methods section. We found that hypoxia significantly induced HIF-1α transcript levels in agreement with previous reports [30, 31], a mechanism that could involve Egr-1 transcriptional regulation of HIF-1α [31]. In support of that assumption, an Egr-1 increase at the protein level during hypoxia was documented by us previously in MSCs [32]. Moreover, *VEGF* and *G6PT* gene expression were also induced, whereas expression of *G6PC-3* and membrane type-1 matrix metalloproteinase (*MT1-MMP*) remained unchanged (Fig. 2A, black bars). Treatment of the cells with $CoCl_2$ also triggered *VEGF* and *G6PT* gene expression, whereas expression of *HIF-1α*, *G6PC-3*, and *MT1-MMP* remained unaffected (Fig. 2A, gray bars). One can conclude that, in the case of $CoCl_2$ treatment, it's not the induction of HIF-1α but the potential blockade of HIF-1α degradation via prolyl hydroxylation and subsequent interaction with Von Hippel-Lindau factor and targeting to proteasomal degradation that may additionally be in play in G6PT regulation. These observations prompted us to analyze the murine *G6PT* gene promoter sequence for the presence of any hypoxia responsive elements (HREs) that could regulate its expression under low oxygen tension. We examined a DNA sequence of 1,207 bp upstream of the ATG start codon (National Center for Biotechnology Information source NM_008063.2) and located on mouse chromosome nine at location 44,205,182-44,211,045 (Fig. 2B). A search for putative transcription factor binding sites was performed with PROMO 3.0 (http://alggen.lsi.upc.es/) using version 8.3 of the TRANSFAC database. A TATA box as well as several previously reported binding

sites were found within the first 200 bp upstream of the ATG and included hepatocyte nuclear factor (HNF)1, HNF3, and CCAAT/enhancer binding protein binding sites [33]. The core consensus sequence of HREs that we searched for was (A/G)CGT(G/C)C and is denoted by asterisks (*) [34]. We found one potential binding site for HIF-1 and two for aryl hydrocarbon receptor (AhR):AhR nuclear translocator (Fig. 2B, boxed). This suggests that possible G6PT transcriptional regulation may occur in MSCs upon hypoxic culture conditions. Whether HIF-1α is involved in such *G6PT* gene regulation was next explored.

Gene Silencing of *HIF-1α* Antagonizes the Effects of Hypoxia on *G6PT* Gene Expression

We used gene silencing strategies to downregulate *HIF-1α* gene expression and to assess its specific contribution to *G6PT* gene regulation under hypoxic culture conditions. MSCs were transiently transfected with scrambled sequences (Mock) or with HIF-1α siRNA as described in the Methods section. Cells were then cultured under normal or hypoxic culture conditions, total RNA was extracted, and qRT-PCR was used to assess *HIF-1α*, *VEGF*, and *MT1-MMP* gene expression. We found that *HIF-1α* gene expression was efficiently reduced in siHIF-1α-transfected cells (Fig. 3A, black bars). *VEGF* gene expression was also reduced in siHIF-1α-transfected cells, and the increase in VEGF expression under hypoxia was reduced by ~58% (Fig. 3A, black bars). *MT1-MMP* gene expression in siHIF-1α-transfected cells remained unaffected. *G6PT* gene expression was also measured in Mock-transfected (Fig. 3B, open circles) and in siHIF-1α-transfected (closed circles) cells that were subsequently cultured under hypoxic conditions (Fig. 3B). Whereas *G6PT* gene expression was transiently increased by hypoxia, with a maximum expression at 10 hours in Mock cells, those cells in which *HIF-1α* gene expression was abrogated were unable to increase *G6PT* gene expression. Consequently, expression of *HIF-1α* is required for G6PT transcriptional regulation upon hypoxia. Since silencing experiments of *HIF-1α* by themselves do not allow one to prove that HIF-1α directly binds to the G6PT promoter, approaches such as chromatin immunoprecipitation assays will be needed. Although the cascade of events may still be indirect, we are confident to have experimentally demonstrated that HIF-1α is a crucial intermediate in the sequence of events that regulate *G6PT* gene expression.

Constitutive Expression of an Oxygen-Dependent Degradation Domain *HIF-1α* Mutant Triggers *G6PT* Gene Expression

In order to recreate the hypoxic culture conditions that trigger *HIF-1α* expression in MSCs, we generated a deletion mutant of *HIF-1α* (HIF-1α [/delta]ODD) and stably transfected MSCs as described in the Methods section. We found that MSCs constitutively and stably expressing HIF-1α [/delta]ODD (MSC-HIF-1α cells) exhibited an increased intrinsic ability to migrate (Fig. 4A). Such increased migratory potential has been documented previously [32] and, although speculative, may potentially involve autocrine regulation through hypoxia-regulated growth factor expression. This may provide efficient mobilization and adaptative behavior of MSCs to an oxygen-deprived environment. When total RNA was extracted from MSCs or MSC-HIF-1α cells, we found that *HIF-1α*, *VEGF*, *MT1-MMP*, and *G6PT* gene expression levels were significantly increased in MSC-HIF-1α cells (Fig. 4B, black bars). In order to confirm that HIF-1α could potentially directly interact with HRE sequences found within the G6PT promoter, we isolated nuclear extracts from MSC-HIF-1α cells

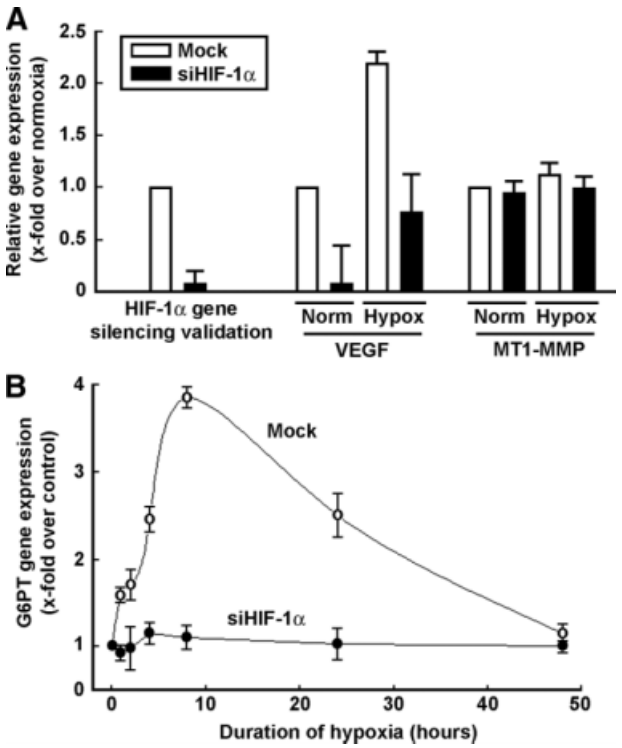

Figure 3. Gene silencing of *HIF-1α* antagonizes the effects of hypoxia on *G6PT* gene expression. **(A):** Mesenchymal stromal cells were transiently transfected with scrambled sequences (Mock, white bars) or HIF-1α siRNA (black bars) as described in the Methods section. Cells were then cultured under normal or hypoxic culture conditions, total RNA was extracted, and qRT-PCR was used to assess *HIF-1α*, *VEGF*, and *MT1-MMP* gene expression as described in Figure 2. **(B):** *G6PT* gene expression was assessed by qRT-PCR in Mock-transfected (open circles) and in siHIF-1α-transfected (closed circles) cells that were subsequently cultured under hypoxic conditions. Abbreviations: G6PT, glucose-6-phosphate transporter; HIF-1α, hypoxia inducible factor 1α; MT1-MMP, membrane type-1 matrix metalloproteinase; qRT-PCR, quantitative reverse transcription-polymerase chain reaction; siRNA, small interfering RNA; VEGF, vascular endothelial growth factor.

and showed that HIF-1α protein was indeed constitutively present within the nuclear fraction of MSC-HIF-1α cells whereas nuclear PARP expression remained constant (Fig. 4C). Electrophoretic mobility assays were also performed in order to demonstrate that nuclear HIF-1α interacted with radiolabeled oligonucleotides (mHIF-1) containing the HIF-1α sequence found within the G6PT promoter. Incubation of the MSC-HIF-1α nuclear extracts with those probes resulted in the formation of three complexes, termed A, B, and C (Fig. 4D, column 1). Complex B and complex C binding to the probe were strongly diminished upon competition with a 25-fold excess of a cold unrelated NSC, suggesting these were non-specific in binding. In contrast, complex A remained intense (Fig. 4D, column 2), but completely disappeared with the same excess of the cold HIF-1α specific competitor or in the presence of an HIF-1α blocking antibody (Fig. 4D, columns 3 and 4).

A Small Molecule G6PT Inhibitor Specifically Triggers Cell Death in MSCs Constitutively Expressing HIF-1α [/delta]ODD

Specific targeting of hypoxic cells such as those found within a tumor microenvironment is a difficult task to achieve. Since

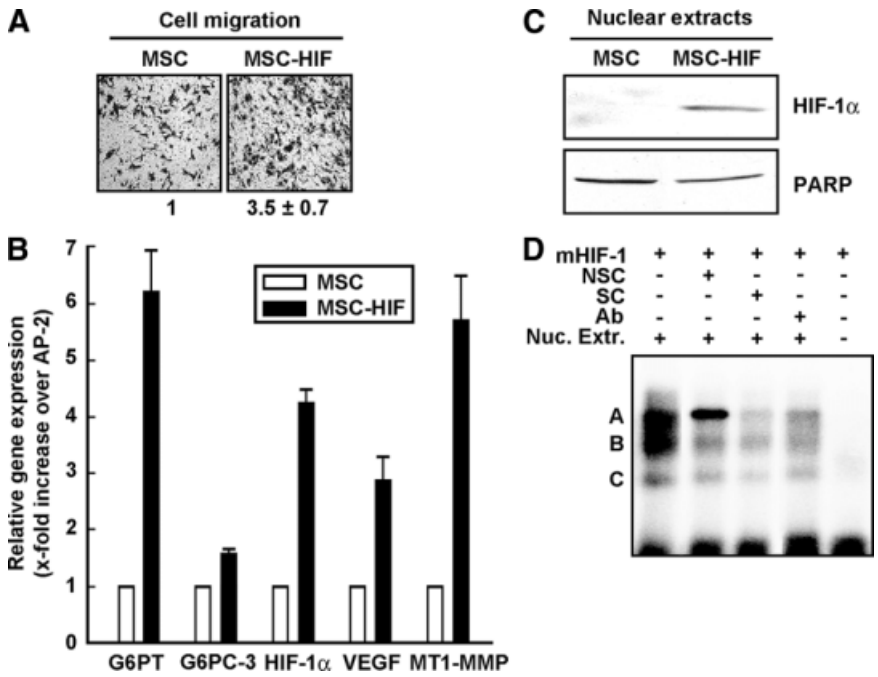

Figure 4. Constitutive expression of an oxygen-dependent degradation domain *HIF-1α* mutant triggers *G6PT* gene expression. **(A):** Basal migration of MSCs and MSCs stably expressing a deletion mutant of *HIF-1α* (HIF-1α [/delta]ODD, MSC-HIF) was performed as described in the Methods section. **(B):** Total RNA was extracted from MSCs (white bars) and MSC-HIF cells (black bars), and quantitative reverse transcription-polymerase chain reaction was performed to assess the gene expression levels of *G6PT*, *G6PC-3*, *VEGF*, *HIF-1α*, and *MT1-MMP*. **(C):** Nuclear extracts were islolated from MSCs and MSC-HIF cells, and Western blotting was performed to detect nuclear HIF-1α or nuclear PARP expression. **(D):** Electrophoretic mobility assays were performed as described in the Methods section using nuclear extracts (Nuc. Extr.) isolated from MSC-HIF cells. Abbreviations: Ab, HIF-1α blocking antibody; G6PC-3, glucose-6-phosphatase catalytic subunit *β*; G6PT, glucose-6-phosphate transporter; HIF-1α, hypoxia inducible factor 1α; MSC, mesenchymal stromal cell; MT1-MMP, membrane type-1 matrix metalloproteinase; NSC, cold unrelated nonspecific competitor; ODD, oxygen-dependent degradation domain; PARP, poly-(ADP-ribose) polymerase; SC, cold HIF-1α specific competitor; VEGF, vascular endothelial growth factor.

we have found that hypoxic MSCs express high levels of G6PT, we hypothesized that these cells would be sensitive to G6PT inhibitors. We used CHL, a natural product with weak G6PT inhibitory activity [35], and a more potent semisynthetic polyketide analog (AD4-015) of a different natural product, mumbaistatin [36] (Fig. 5A). Dose–response curves for G6PT inhibition by AD4-015 in both rat liver microsomal assays as well as hepatocyte assays were reported earlier [36]. In the microsomal assay, the 50% inhibitory concentration was 2.5 μM, whereas in the cell-based assay, inhibition was only observed at 10-fold higher concentrations, a feature that is constant with all known G6PT inhibitors and is presumably a reflection of target access [36]. Because that cell-based assay more accurately reflects our own MSC assays, we used a concentration of 25 μM in the current assays. MSCs and MSC-HIF-1α cells were thus treated with 100 μM CHL or 25 μM AD4-015, and cell death was assessed. We found that greater Hoechst staining (apoptosis) as well as PI staining (necrosis) was observed in treated MSC-HIF-1α cells in comparison with MSCs (Fig. 5B). Cell death was not significantly induced by CHL, whereas AD4-015 triggered approximately three times more cell death in MSC-HIF-1α cells (Fig. 5C). In support of the prosurvival phenotype ascribed to MSC-HIF cells, their basal levels of phospho-AKT and phospho-ERK protein expression were found to be greater than those of MSCs (Fig. 5D). Treatment of the cells with AD4-015 was found to specifically downregulate phospho-AKT expression levels in MSC-HIF cells but not in MSCs (Fig. 5D), suggestive of targeted cell death induction in MSC-HIF cells. Altogether, these data suggest that small molecule inhibitors of G6PT may show selectivity in targeting hypoxic MSCs.

Discussion

Most commonly isolated from the bone marrow, MSCs are multipotent adult stem cells with immunomodulatory effects and the ability to home to sites of injury. These properties, although clearly useful for therapeutic purposes, may, however, be used by cancer cells for their own ends. Indeed, as the importance of the microenvironment and stroma to the evolution and progression of solid tumors has been revealed over the past few years, MSCs that are the progenitors of stromal cells and fibroblasts have been found to interact with cancer cells [37]. In fact, the homing of MSCs to tumors is thought to be the earliest phenomenon of MSC–cancer interactions, as was recently reported in a mouse model where injected human MSCs could be found preferentially migrating to implanted human melanoma tumors [5]. Subsequently, studies have shown MSCs homing to tumors and even to sites of metastasis [38]. Furthermore, cotransplantation of MSCs with melanoma cells in mice enhanced tumor engraftment and growth [39]. These data are in agreement with our own observations that vascular progenitors derived from bone marrow stromal cells are recruited by tumors both in vivo and in vitro [7]. Collectively, the sum of this evidence, in line with the increased ability of MSCs to migrate under an atmosphere of low oxygen, as is seen in the tumor microenvironment [32], suggests that MSCs are active participants in the development of solid tumors.

The expression of a number of glycolytic isozymes (e.g., liver-type phosphofructokinase-1, aldolase A, aldolase C, phosphoglycerate kinase 1, enolase 1, and lactate dehydrogenase

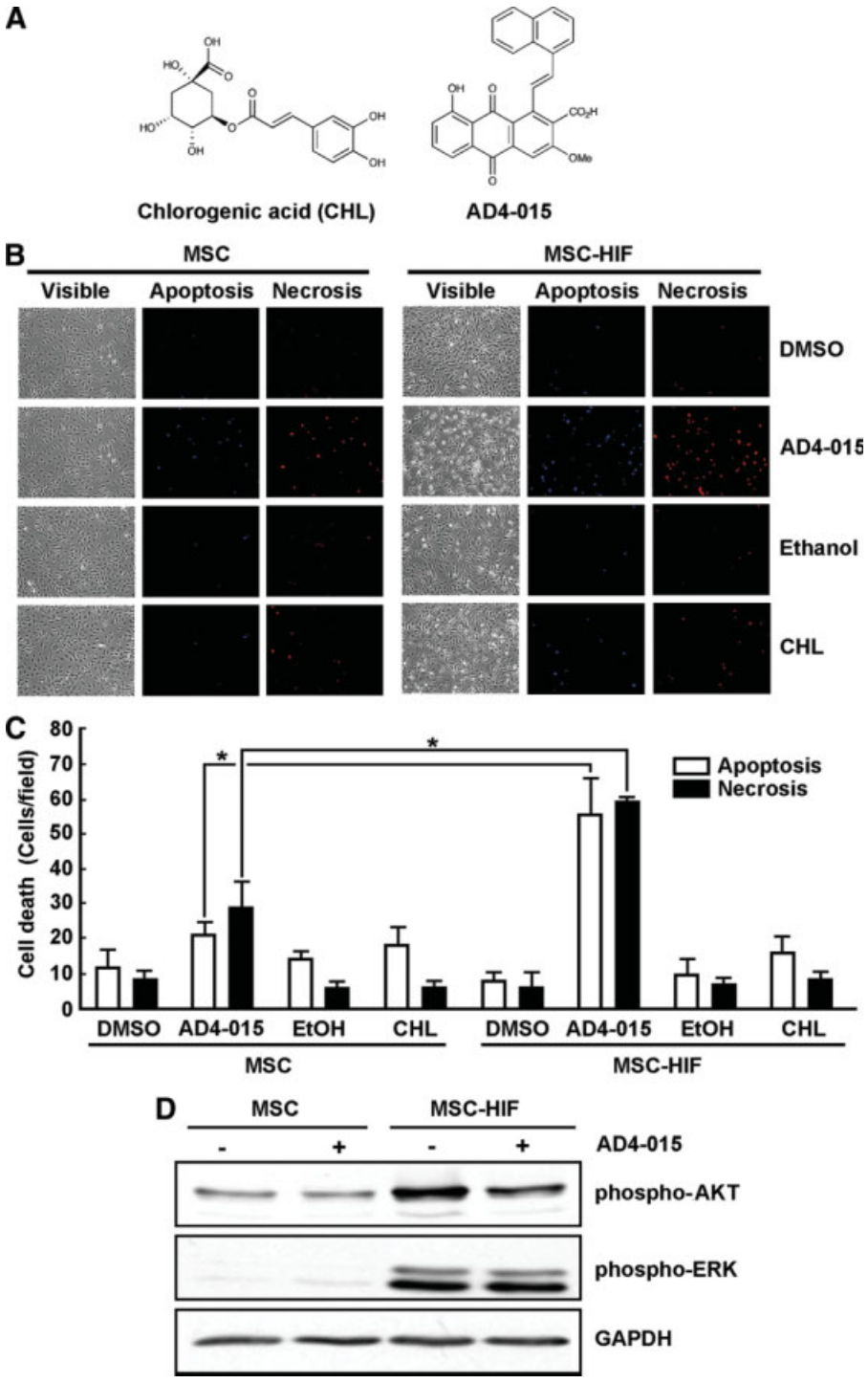

Figure 5. The mumbaistatin analog and potent G6PT inhibitor AD4-015 specifically triggers cell death in MSCs constitutively expressing HIF-1α [/delta]ODD. **(A):** Chemical structures of CHL and the mumbaistatin analog AD4-015. **(B):** MSCs or MSC-HIF cells were cultured under normoxic conditions then treated for 18 hours with 25 μM AD4-015 (or respective DMSO), or with 100 μM CHL (or respective EtOH vehicle). Hoechst (apoptosis) and propidium iodide (necrosis/late apoptosis) cell labeling was then performed and visualized using fluorescence microscopy. **(C):** Quantification was performed by visual counting. The mean of four fields from three independent experiments is shown. Probability values of less than 0.05 were considered significant, and an asterisk identifies such significance. **(D):** MSCs and MSC-HIF cells were treated with AD4-015 as in **(B)** and lysates were isolated. SDS-PAGE followed by immunodetection of phospho-ERK, phospho-AKT, or GAPDH was performed as described in the Methods section. Abbreviations: CHL, chlorogenic acid; DMSO, dimethylsulfoxide vehicle; ERK, extracellular signal related kinase; EtOH, ethanol; G6PT, glucose-6-phosphate transporter; GAPDH, glyceraldehyde-3-phosphate dehydrogenase; HIF-1α, hypoxia inducible factor 1α; MSC, mesenchymal stromal cell; ODD, oxygen-dependent degradation domain.

A) has already been found to be induced by hypoxia in a tissue-specific manner [40, 41]. Analysis of the *cis*-acting sequences of these genes has revealed that hypoxia-induced activation requires binding sites for HIF-1. All the above genes, together with *G6PT*, reflect the adaptative capacity of MSCs to oxygen deprivation. Pharmacological targeting of G6PT functions, and hence induction of possible glucose deprivation conditions, should thus be deleterious to the hypoxic cell, as denoted by our own data in Figures 5B and 5D, where cell death was specifically triggered. In this report, we have undertaken a detailed study to delineate the role of G6PT that could link metabolic and survival adaptation to hypoxia in MSCs. Through the generation of an MSC-HIF-1α stable cell line and through the use of siRNA gene silencing strategies, we also showed that HIF-1α is involved in the transcriptional regulation of G6PT. As a consequence, *G6PT* gene expression was increased by hypoxia, supporting a prosurvival role for G6PT. In agreement with this observation, G6PT-deficient neutrophils isolated from GSD-Ib mice are characterized by increased rates of apoptosis [42], possibly consequent to increased expression of ER stress-related, glucose-regulated proteins and protein disulfide isomerase [43, 44]. These

findings are thus in agreement with the ubiquitous expression and prosurvival functions of G6PT that were reported in glioma cells and in MSCs [18, 24]. Investigation of whether increased G6PT functions could potentially affect the glycolytic phenotype and make hypoxic MSCs gluconeogenic must also be considered in the metabolic adaptation phenotype to hypoxia.

Alternate G6PT roles, distinct from its classic involvement in the G6Pase system, include ATP-mediated calcium sequestration in the ER lumen [45], activity as a G6P receptor/sensor [46], and supplying G6P to a ubiquitously expressed luminal glucose-6-phosphate dehydrogenase [47]. One or more of these functions may also be responsible for crucial prosurvival processes, including tumor cell proliferation, cell cycle division, and extracellular matrix degradation. In fact, the observed increases in MSC-HIF cells of ERK phosphorylation and AKT phosphorylation correlate with the high migratory and prosurvival phenotype observed. Our current study thus supports these functions of the ubiquitously expressed G6PT in nongluconeogenic tissues. Furthermore, the luminal hexose-6-phosphate dehydrogenase also provides reducing equivalents needed for several important reductases that protect the ER against damage by reactive oxygen species. Lack of protection may result in premature cell death through apoptosis.

In light of the role of G6PT in MSC biology that has been highlighted by our results, selective interference with G6PT functions and/or expression may be an attractive therapeutic approach to metabolic control of cancer cell growth or in preventing circulating cells from being recruited to contribute to tumor development. Indeed, gene silencing of *G6PT* has already been shown to suppress intracellular signaling that leads to calcium mobilization by sphingosine-1-phosphate [23], a potent bioactive lipid and inducer of MSC mobilization [27]. Here, we further demonstrate that the small molecule G6PT inhibitor AD4-015 can induce apoptosis and necrosis of hypoxic MSCs (MSC-HIF-1α cells) that show high sustained endogenous *G6PT* gene expression. Noteworthy, treatment of MSCs under hypoxic conditions with AD4-015 did not result in any difference in cell death, most probably because *G6PT* gene expression is transient, peaking at $\sim$8 hours of hypoxia (Fig. 3B). We believe that our MSC-HIF-1α model better reflects the long-term metabolic adaptation of the cells to hypoxia and highlights the specific contribution of HIF-1α to *G6PT* gene expression. Altogether, this may provide some rationale for a potentially new therapeutic action against hypoxic cells embedded within tumors.

Since studies have so far been limited to a few types of cancers, it is still unknown how MSCs interact with other cancers, if at all. Whether the animal models used accurately reflect what actually occurs within the hypoxic tumor setting remains to be established, because most in vivo experiments use high numbers of exogenously introduced MSCs, an unlikely scenario in the endogenous state. Still, exogenously delivered human MSCs were reported to specifically localize to human gliomas after intravascular delivery [6], which raises the possibility that endogenous MSCs may be recruited into hypoxic gliomas during tumorigenesis and may contribute to the physiological growth of brain tumors in situ. Preliminary data from our own work also demonstrate high *G6PT* expression levels within experimental hypoxic brain tumors (data not shown). Furthermore, tumor-derived MSCs were recently isolated and characterized as $CD133^-$ cells, indicating that they are distinct from classic $CD133^+$ glioma cancer stem cells. These $CD133^-$ MSCs were more commonly isolated from high-grade tumors than from low-grade gliomas, supporting the hypothesis that tumor-derived MSCs are involved in glioma progression from low to high grade [48]. Accordingly, extremely low $CD133^-$ glioblastomas were found to show a mesenchymal subclass-like gene expression profile, which has the worst clinical outcome [49].

In conclusion, our study reveals a potential metabolic adaptation of MSCs to hypoxic conditions that enables them to survive under conditions characterized by low oxygen levels and glucose deprivation, such as is found within developing tumors. Such metabolic flexibility may, in part, be accounted for by the prosurvival functions of G6PT that would allow these MSCs to contribute to tumor development. More importantly, hypoxic MSCs that contribute to tumor development may also be selectively targeted by small molecule G6PT inhibitors such as the semisynthetic polyketide derivative AD4-015, modeled after the natural product mumbaistatin.

Acknowledgments

B.A. holds a Canada Research Chair in Molecular Oncology from the Canadian Institutes of Health Research (CIHR). This study was funded by a grant from the U.S. National Institutes of Health to C.K. (CA 77248), and by a grant of the Natural Sciences and Engineering Research Council of Canada (NSERC) to B.A.

Disclosure of Potential Conflicts of Interest

The authors indicate no potential conflicts of interest.

References

1 Tso CL, Shintaku P, Chen J et al. Primary glioblastomas express mesenchymal stem-like properties. Mol Cancer Res 2006;4:607–619.
2 Kaur B, Khwaja FW, Severson EA et al. Hypoxia and the hypoxia-inducible-factor pathway in glioma growth and angiogenesis. Neuro Oncol 2005;7:134–153.
3 Prockop DJ. Marrow stromal cells as stem cells for nonhematopoietic tissues. Science 1997;276:71–74.
4 Horwitz EM, Le Blanc K, Dominici M et al. The International Society for Cellular Therapy. Clarification of the nomenclature for MSC: The International Society for Cellular Therapy position statement. Cytotherapy 2005;7:393–395.
5 Studeny M, Marini FC, Champlin RE et al. Bone marrow-derived mesenchymal stem cells as vehicles for interferon-beta delivery into tumors. Cancer Res 2002;62:3603–3608.
6 Nakamizo A, Marini F, Amano T et al. Human bone marrow-derived mesenchymal stem cells in the treatment of gliomas. Cancer Res 2005;65:3307–3318. Erratum in: Cancer Res 2006;66:5975.
7 Annabi B, Naud E, Lee YT et al. Vascular progenitors derived from murine bone marrow stromal cells are regulated by fibroblast growth factor and are avidly recruited by vascularizing tumors. J Cell Biochem 2004;91:1146–1158.
8 Birnbaum T, Roider J, Schankin CJ et al. Malignant gliomas actively recruit bone marrow stromal cells by secreting angiogenic cytokines. J Neurooncol 2007;83:241–247.
9 Mylotte LA, Duffy AM, Murphy M et al. Metabolic flexibility permits mesenchymal stem cell survival in an ischemic environment. Stem Cells 2008;26:1325–1336.
10 Hers HG. Mechanisms of blood glucose homeostasis. J Inherit Metab Dis 1990;13:395–410.
11 Bartrons R, Caro J. Hypoxia, glucose metabolism and the Warburg's effect. J Bioenerg Biomembr 2007;39:223–229.

12 Patiar S, Harris AL. Role of hypoxia-inducible factor-1alpha as a cancer therapy target. Endocr Relat Cancer 2006;13(suppl 1):S61–S75.
13 Du R, Lu KV, Petritsch C et al. HIF1alpha induces the recruitment of bone marrow-derived vascular modulatory cells to regulate tumor angiogenesis and invasion. Cancer Cell 2008;13:206–220.
14 Ceradini DJ, Gurtner GC. Homing to hypoxia: HIF-1 as a mediator of progenitor cell recruitment to injured tissue. Trends Cardiovasc Med 2005;15:57–63.
15 Kim SY, Nguyen AD, Gao JL et al. Bone marrow-derived cells require a functional glucose 6-phosphate transporter for normal myeloid functions. J Biol Chem 2006;281:28794–28801.
16 Yiu WH, Pan CJ, Allamarvdasht M et al. Glucose-6-phosphate transporter gene therapy corrects metabolic and myeloid abnormalities in glycogen storage disease type Ib mice. Gene Ther 2007;14:219–226.
17 Belkaid A, Currie JC, Desgagnés J et al. The chemopreventive properties of chlorogenic acid reveal a potential new role for the microsomal glucose-6-phosphate translocase in brain tumor progression. Cancer Cell Int 2006;6:7.
18 Currie JC, Fortier S, Sina A et al. MT1-MMP down-regulates the glucose 6-phosphate transporter expression in marrow stromal cells: A molecular link between pro-MMP-2 activation, chemotaxis, and cell survival. J Biol Chem 2007;282:8142–8149.
19 Chou JY, Matern D, Mansfield BC et al. Type I glycogen storage diseases: Disorders of the glucose-6-phosphatase complex. Curr Mol Med 2002;2:121–143.
20 Chen LY, Shieh JJ, Lin B et al. Impaired glucose homeostasis, neutrophil trafficking and function in mice lacking the glucose-6-phosphate transporter. Hum Mol Genet 2003;12:2547–2558.
21 Leuzzi R, Bánhegyi G, Kardon T et al. Inhibition of microsomal glucose-6-phosphate transport in human neutrophils results in apoptosis: A potential explanation for neutrophil dysfunction in glycogen storage disease type 1b. Blood 2003;101:2381–2387.
22 Cheung YY, Kim SY, Yiu WH et al. Impaired neutrophil activity and increased susceptibility to bacterial infection in mice lacking glucose-6-phosphatase-beta. J Clin Invest 2007;117:784–793.
23 Fortier S, Labelle D, Sina A et al. Silencing of the MT1-MMP/G6PT axis suppresses calcium mobilization by sphingosine-1-phosphate in glioblastoma cells. FEBS Lett 2008;582:799–804.
24 Belkaid A, Copland IB, Massillon D et al. Silencing of the human microsomal glucose-6-phosphate translocase induces glioma cell death: Potential new anticancer target for curcumin. FEBS Lett 2006; 580:3746–3752.
25 Belkaid A, Fortier S, Cao J et al. Necrosis induction in glioblastoma cells reveals a new "bioswitch" function for the MT1-MMP/G6PT signaling axis in proMMP-2 activation versus cell death decision. Neoplasia 2007;9:332–340.
26 van de Werve G, Lange A, Newgard C et al. New lessons in the regulation of glucose metabolism taught by the glucose 6-phosphatase system. Eur J Biochem 2000;267:1533–1549.
27 Meriane M, Duhamel S, Lejeune L et al. Cooperation of matrix metalloproteinases with the RhoA/Rho kinase and mitogen-activated protein kinase kinase-1/extracellular signal-regulated kinase signaling pathways is required for the sphingosine-1-phosphate-induced mobilization of marrow-derived stromal cells. Stem Cells 2006;24:2557–2565.
28 Dignam JD, Lebovitz RM, Roeder RG. Accurate transcription initiation by RNA polymerase II in a soluble extract from isolated mammalian nuclei. Nucleic Acids Res 1983;11:1475–1189.
29 Benson BA, Butler YX, Ackerman M et al. A kinase/phosphatase system involving the protooncogene Lck is necessary for inducible modulation of Sob 1 during T cell activation. Cell Immunol 1996;170: 245–250.
30 Belaiba RS, Bonello S, Zahringer C et al. Hypoxia up-regulates hypoxia-inducible factor-1alpha transcription by involving phosphatidylinositol 3-kinase and nuclear factor kappaB in pulmonary artery smooth muscle cells. Mol Biol Cell 2007;18:4691–4697.
31 Sperandio S, Fortin J, Sasik R et al. The transcription factor Egr1 regulates the HIF-1alpha gene during hypoxia. Mol Carcinog 2008;48: 38–44.
32 Annabi B, Lee YT, Turcotte S et al. Hypoxia promotes murine bone-marrow-derived stromal cell migration and tube formation. Stem Cells 2003;21:337–347.
33 Hiraiwa H, Pan CJ, Lin B et al. A molecular link between the common phenotypes of type 1 glycogen storage disease and HNF1α-null mice. J Biol Chem 2001;276:7963–7967.
34 Kimura H, Weisz A, Ogura T et al. Identification of hypoxia-inducible factor 1 ancillary sequence and its function in vascular endothelial growth factor gene induction by hypoxia and nitric oxide. J Biol Chem 2001;276:2292–2298.
35 Hemmerle H, Burger HJ, Below P et al. Chlorogenic acid and synthetic chlorogenic acid derivatives: Novel inhibitors of hepatic glucose-6-phosphate translocase. J Med Chem 1997;40:137–145.
36 Lee TS, Das A, Khosla C. Structure-activity relationships of semisynthetic mumbaistatin analogs. Bioorg Med Chem 2007;15:5207–5218.
37 Yen BL, Yen ML. Mesenchymal stem cells and cancer—for better or for worse?J Cancer Mol 2008;4:5–9.
38 Dwyer RM, Potter-Beirne SM, Harrington KA et al. Monocyte chemotactic protein-1 secreted by primary breast tumors stimulates migration of mesenchymal stem cells. Clin Cancer Res 2007;13:5020–5027.
39 Djouad F, Plence P, Bony C et al. Immunosuppressive effect of mesenchymal stem cells favors tumor growth in allogeneic animals. Blood 2003;102:3837–3844.
40 Semenza GL, Roth PH, Fang HM et al. Transcriptional regulation of genes encoding glycolytic enzymes by hypoxia-inducible factor 1. J Biol Chem 1994;269:23757–23763.
41 Ebert BL, Gleadle JM, O'Rourke JF et al. Isoenzyme-specific regulation of genes involved in energy metabolism by hypoxia: Similarities with the regulation of erythropoietin. Biochem J 1996;313:809–814.
42 Kuijpers TW, Maianski NA, Tool AT et al. Apoptotic neutrophils in the circulation of patients with glycogen storage disease type 1b (GSD1b). Blood 2003;101:5021–5024.
43 Lee AS. The glucose-regulated proteins: Stress induction and clinical applications. Trends Biochem Sci 2001;26:504–510.
44 Schröder M, Kaufman RJ. The mammalian unfolded protein response. Annu Rev Biochem 2005;74:739–789.
45 Chen PY, Csutora P, Veyna-Burke NA et al. Glucose-6-phosphate and Ca2+ sequestration are mutually enhanced in microsomes from liver, brain, and heart. Diabetes 1998;47:874–881.
46 Hiraiwa H, Pan CJ, Lin B et al. Inactivation of the glucose 6-phosphate transporter causes glycogen storage disease type 1b. J Biol Chem 1999;274:5532–5536.
47 van Schaftingen E, Gerin I. The glucose-6-phosphatase system. Biochem J 2002;362:513–532.
48 Lang FF, Amano T, Hata N et al. Tumor-derived mesenchymal stem cells in human gliomas: Isolation and biological effects. Presented at the 2008 American Association for Cancer Research Annual Meeting, San Diego, April 12-16, 2008.
49 Joo KM, Kim SY, Kim MH et al. CD133-negative glioblastoma cancer stem cells represent the 'mesenchymal' subclass of glioblastoma. Presented at the 2008 American Association for Cancer Research Annual Meeting,San Diego, April 12-16, 2008.
50 Messeguer X, Escudero R, Farré D et al. PROMO: Detection of known transcription regulatory elements using species-tailored searches. Bioinformatics 2002;18:333–334.
51 Farré D, Roset R, Huerta M et al. Identification of patterns in biological sequences at the ALGGEN server: PROMO and MALGEN. Nucleic Acids Res 2003;31:3651–3653.